Materials Today Bio 23 (2023) 100806

Contents lists available at ScienceDirect

Materials Today Bio

journal homepage: www.journals.elsevier.com/materials-today-bio

Double-layer adhesives for preventing anastomotic leakage and reducing post-surgical adhesion

Sung Il Kang [a], Hyun Ho Shin [b], Da Han Hyun [c], Ghilsuk Yoon [d], Jun Seok Park [e,**], Ji Hyun Ryu [b,f,g,*]

[a] Department of Surgery, College of Medicine, Yeungnam University, Daegu, 42415, South Korea
[b] Department of Chemical Engineering, Wonkwang University, Iksan, Jeonbuk, 54538, South Korea
[c] Department of Biomedical Science, School of Medicine, Kyungpook National University, Daegu, 41404, South Korea
[d] Department of Pathology, School of Medicine, Kyungpook National University, Daegu, 41566, South Korea
[e] Department of Surgery, School of Medicine, Kyungpook National University Hospital, Daegu, 41404, Republic of Korea
[f] Department of Carbon Convergence Engineering, Wonkwang University, Iksan, Jeonbuk, 54538, South Korea
[g] Smart Convergence Materials Analysis Center, Wonkwang University, Iksan, Jeonbuk, 54538, South Korea

ARTICLE INFO

Keywords:
Intestinal anastomosis
Colorectal cancer
Gallic acid-conjugated chitosan
Crosslinked hyaluronic acid
Double layer

ABSTRACT

Preventing anastomotic leakage (AL) and postoperative adhesions after gastrointestinal surgery is crucial for ensuring a favorable surgical prognosis. However, AL prevention using tissue adhesives can unintentionally lead to undesirable adhesion formation, while anti-adhesive agents may interfere with wound healing and contribute to AL. In this study, we have developed a double-layer patch, consisting of an adhesive layer on one side, utilizing gallic acid-conjugated chitosan (CHI-G), and an anti-adhesive layer on the opposite side, employing crosslinked hyaluronic acid (cHA). These CHI-G/cHA double-layer adhesives significantly prevented AL by forming physical barriers of CHI-G and reduced post-surgical adhesion at the anastomosis sites by the anti-adhesive layers of cHA. The bursting pressure (161.1 ± 21.6 mmHg) of double-layer adhesives-applied rat intestine at postoperative day 21 was far higher than those of the control (129.4 ± 5.7 mmHg) and the commercial anti-adhesives-applied group (120.8 ± 5.2 mmHg). In addition, adhesion score of double-layer adhesives-applied rat intestine was 3.6 ± 0.3 at postoperative day 21, which was similar to that of the commercial anti-adhesives-applied group (3.6 ± 0.3) and lower than that of the control group (4.9 ± 0.5). These findings indicate that the double-layer patch (CHI-G/cHA) has the potential to effectively prevent both postoperative adhesions and anastomotic leakage, offering a promising solution for gastrointestinal surgery.

1. Introduction

Anastomotic leakage (AL) is a serious complication of gastrointestinal surgery. The well-known potential risk factors of AL are patients' medical conditions, surgical techniques, radiation exposure, and anastomotic organs [1–4]. For instance, the overall incidence of AL after ileocolic anastomosis is 0.4–6.5% [1–4], whereas the incidence of AL after rectal resection was up to 30% [5]. Prevention of AL during surgical procedures is important because it is associated with high morbidity and mortality [1–4,6]. When AL occurs, reoperation and/or intervention is required to ensure patient safety, which inevitably increases medical expenses [7,8]. Thus, developing adhesive materials that can act as adjuncts for anastomosis via effectively sealing the anastomotic sites is highly desirable to prevent AL.

Several tissue adhesives are currently being developed in response to these clinical requirements, and a few of them are already in the market and currently utilized in clinical settings. Although the sealing effect of tissue adhesives such as cyanoacrylate, acrylate, gelatin, collagen, and fibrin glues for preventing AL in clinical practice is ambiguous, several experimental and animal studies have reported promising results [9–11]. For instance, cyanoacrylate-based tissue adhesives (i.e., ethyl-cyanoacrylate, N-butyl-cyanoacrylate, iso-butyl-cyanoacrylate, and 2-octyl-cyanoacrylate) reduce AL by sealing anastomosis sites via rapid polymerization [12,13]. Cyanoacrylates exhibit excellent

* Corresponding author. Department of Carbon Convergence Engineering, Wonkwang University, Iksan, Jeonbuk, 54538, South Korea.
** Corresponding author. Department of Surgery, School of Medicine, Kyungpook National University Hospital, Daegu, 41404, South Korea.
E-mail addresses: parkjs0802@knu.ac.kr (J.S. Park), jhryu4816@wku.ac.kr (J.H. Ryu).

https://doi.org/10.1016/j.mtbio.2023.100806
Received 10 June 2023; Received in revised form 6 September 2023; Accepted 18 September 2023
Available online 20 September 2023

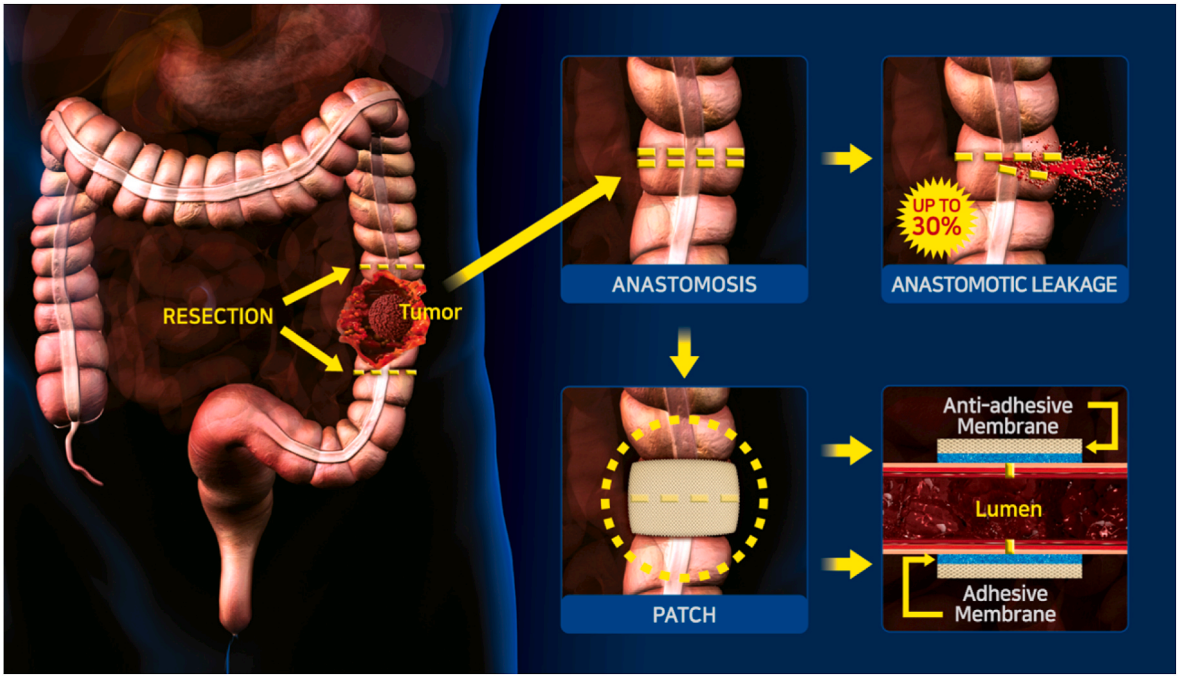

Fig. 1. Schematic illustration of the role of double-layer adhesives for intestinal anastomosis. In general, anastomotic leakage occurred in up to 30% cases after resection of colorectal cancers. The double-layer adhesive prevents anastomotic leakage with the reduction of post-surgical adhesions.

mechanical and adhesive properties *in vitro* [14]. However, the effects of cyanoacrylate after suturing of colonic anastomotic sites may be negative during anastomotic healing, as previously reported [15,16]. In addition, safety issues related to direct tissue damage during curing reactions and toxic degradation products that are not suitable for medical applications remain [15,16]. Fibrin glue-based tissue adhesives significantly increase anastomotic bursting pressures by sealing AL sites in rat models [17]. Fibrin glue promotes fibrous healing with low inflammation, resulting in the prevention of AL during colonic anastomosis [18]. Similar to fibrin glues, gelatin [19–21], collagen [22–24], chitosan [25,26], lectin [27], and synthetic adhesives [28] with slight modifications, combinations, and forms/shapes, are used as sealing materials to prevent AL. The effectiveness of several tissue adhesive materials in anastomosis has been reported; however, further studies are required to provide convincing evidence for their clinical use in surgical procedures.

Tissue adhesives have the potential to reinforce anastomotic sites and prevent AL. Conversely, this capability can also result in excessive adhesion, potentially contributing to intestinal obstruction [22]. Indeed, the adhesion formation index of the group treated with tissue adhesives was higher than that of the normal group in our previous study [29]. Postoperative intestinal adhesions are primarily caused by surgical trauma. In addition, postoperative adhesions are the most common complications of abdominal or pelvic surgery, and completely preventing adhesions in patients who undergo gastrointestinal or pelvic surgery is almost impossible [30]. The incidence of symptomatic postoperative adhesions occurring within one month after surgery has been reported to vary, with rates ranging from less than 1%–26% [31]. Intestinal adhesions are also clinically significant because they can lead to acute or chronic abdominal pain, intestinal obstruction, and symptoms that require hospitalization or reoperation. Therefore, in the case that tissue adhesives may induce intestinal adhesions, they should be approached with caution, and such side effects must be minimized.

Phenolic compound-conjugated polymers have been extensively synthesized for various biomedical applications [32,33]. The conjugation of catechol or gallol groups to polymeric backbones enhances water-resistant tissue adhesive properties, retaining the intrinsic properties of the polymers. In addition, double-layered patches and hydrogels have recently been developed for tissue repair to prevent tissue adhesion [34–38]. For instance, double-layer adhesives of mussel-inspired hydrogels with an anti-adhesive layer stably adhere to cardiac tissues that are effective in repairing myocardial infarction and preventing tissue adhesions [34]. Also, double-layer hydrogels composed of the adhesive layers with transglutaminase-crosslinked gelatin and alginate hydrogels and the anti-adhesive layers of alginate and carboxymethyl cellulose composites shows the promotion of wound healings and prevention of a partial hepatectomy-induced adhesions [35]. Thus, the rational design of biomaterials with opposing characteristics provides efficient strategies for versatile biomedical applications in many surgeries.

Our hypothesis postulates that a bilayer material comprising an adhesive layer on one side and an anti-adhesive layer on the opposite side can prevent AL while alleviating concerns of post-surgical adhesion in relation to tissue adhesive usage. We expect that the adhesive layer of patches can prevent leakage by sealing undesirable perforation sites and the anti-adhesive layers can reduce post-surgical adhesion, as shown in Fig. 1. In this study, we developed a double-layer adhesive consisting of gallic acid-conjugated chitosan (CHI-G) as the adhesive material and crosslinked hyaluronic acid (cHA) as the anti-adhesive material for intestinal anastomosis. The CHI-G/cHA double-layer adhesive exhibited an excellent sealing performance and reduced the occurrence of unintentional adhesion when tissue adhesive materials were used in the large intestine (cecum) as an AL animal model. AL is more prevalent in colon and rectal surgeries than in surgeries involving the small intestine or stomach in clinical practice. In addition, the surgeries were performed with sutures using a loose suture technique that created an AL model that closely resembled an actual clinical scenario. Thus, this study demonstrates the possibility of using CHI-G/cHA double-layer adhesives to prevent AL and reduce post-surgical adhesions.

2. Materials and methods

2.1. Materials

Chitosan (medium molecular weight, 200–800 cp, 75–85% deacetylated) and gallic acid were purchased from Sigma-Aldrich (USA). 1-Ethyl-3-(3-dimethylaminopropyl)-carbodiimide hydrochloride (EDC) was purchased from TCI-SU (Japan). HA (M.W. 1 MDa) was purchased from LifeCore (USA). Acetone (Daejung Chemical, Republic of Korea) was used as received without further purification. All other chemicals were of analytical grade.

2.2. Synthesis of CHI-G

CHI-G was synthesized using standard carbodiimide chemistry. Briefly, chitosan (1 g) was dissolved in pH 5.0 HCl solution (100 mL). Gallic acid (1.1 g) and EDC (1.2 g) in a co-solvent (50 mL) of DDW and ethanol (1:1 v/v) were added to the chitosan solution, and the pH was adjusted to 5.0. The reaction time was 12 h and the pH of the reaction solution was maintained during the reaction. The product was dialyzed using a membrane (MWCO = 3.5 kDa, SpectraPor) against a pH 2.0 NaCl solution (10 mM) for 2 days and DDW for 4 h. The final product was then lyophilized. CHI-G synthesis was confirmed by ^{1}H NMR (Bruker Avance, 500 MHz) and UV–Vis spectroscopy (UV-1900i, Shimadzu). The degree of gallol substitution by CHI-G was estimated by comparing its absorbance at 265 nm caused by the gallol groups with the standard curves of gallic acid concentrations. The degree of gallol substitution was calculated as 6.0 ± 0.9%.

2.3. Preparation of CHI-G/cHA double-layer adhesives

CHI-G/cHA double-layer adhesives were fabricated using a simple freeze-drying method. Briefly, HA (1.5 wt%) was dissolved in DDW, poured into freeze-dried molds, and lyophilized. To crosslink HA, EDC in acetone (2 mg/mL) and DDW washing solutions were prepared. After lyophilization, the HA patches were soaked in EDC solution (50 mL) for 24 h and washed thrice with DDW solution. The crosslinked HA patches (cHA) were placed on freeze-dried molds and frozen at −20 °C. The CHI-G solution (1.5 wt%) was poured onto the frozen cHA patches and both were lyophilized. The morphological differences of CHI-G and cHA layers with interfaces between two layers were monitored using scanning electron microscopy (SEM, S-4800, Hitachi Ltd., Tokyo, Japan) at an acceleration voltage of 15 kV at the Core Facility for Supporting Analysis & Imaging of Biomedical Materials at Wonkwang University, which is supported by the National Research Facilities and Equipment Center.

2.4. Study on swelling ratio and stability of CHI-G/cHA double-layer adhesives

To measure the swelling ratios, cHA, CHI-G, and CHI-G/cHA double-layer patches were prepared. The patches (*ca.* 20 mg) were placed in a PBS solution (pH 7.4, 1 mL) and maintained for 21 days at 37 °C. At predetermined time intervals (0.04, 0.13, 0.25, 0.5, 1, 2, 3, 5, 7, 14, and 21 days), the swelling ratios were measured after removing the PBS solution with surface moisture using the following equations:

$$Swelling\ ratio\ (\%) = \frac{w_{wet} - w_{dry}}{w_{dry}} \times 100\ \left(\%\right)$$

In addition, *in vitro* stabilities of cHA, CHI-G, and CHI-G/cHA double-layer patches were monitored in PBS (pH 7.4) solution. In brief, patches (*ca.* 20 mg) were placed in the PBS solution (pH 7.4, 1 mL) and incubated for 21 days at 37 °C. At predetermined time intervals (1, 2, 3, 5, 7, 14, and 21 days), the supernatants were removed, washed with DDW, and lyophilized. After fully drying, the remaining weight (W_t) of each patch was measured. *In vitro* stabilities of cHA, CHI-G, and CHI-G/cHA double-layer patches were calculated using the following equation:

$$Remaining\ weight\ (\%) = \frac{w_t}{w_{initial}} \times 100\ \left(\%\right)$$

The measurements of *in vitro* stabilities were performed in triplicates.

To monitor *in vivo* stabilities, CHI-G/cHA double-layer patches (25 ± 0.5 mg) were implanted on the anastomosis sites of rats. At predetermined time intervals (3, 7, 21 days), the hydrogel patches were collected from the anastomosis sites, and the remaining weights were measured in wet conditions. Also, the remaining weights of patches after lyophilization were measured. The measurements were performed in quadruplicates.

2.5. Tissue adhesive properties of CHI-G/cHA double-layer adhesives

To measure the tissue adhesive properties of the CHI-G/cHA double-layer adhesives, a modified lap-shear test was performed using a universal testing machine (UTM, Instron 5583, Instron) with a 50 N load cell. For tissue-adhesion tests, cHA, CHI-G, and CHI-G/cHA double-layer patches were prepared. Briefly, the patches and porcine intestines were cut into 1 × 1 cm^2 square shapes. Polyethylene terephthalate (PET) films were cut into 1 × 5 cm^2 rectangular shapes. Porcine tissues and patches were attached to the edges of the PET films. For the CHI-G/cHA double-layer adhesives, both cHA and CHI-G layers were attached to PET films. The porcine tissue and patches were overlapped and fixed on either side of the UTM holders. Tensile strength was measured by pulling the UTM probe at a loading rate of 1 mm/min. All measurements were performed in triplicates.

2.6. In vitro bursting pressure measurements

The bursting pressure of the CHI-G/cHA double-layer adhesive was measured using bursting-pressure monitoring devices equipped with a plastic container, indicator, pressure transmitter, and recorder. Briefly, the porcine intestine was placed in containers and perforated using 3 mm biopsy punches and 18-gauge needles, respectively. The CHI-G/cHA double-layer adhesive was cut into a round shape with a diameter of 15 mm. The CHI-G/cHA double-layer adhesives were attached to the perforation site of the intestine, and air was blown into the container. The pressure was monitored when a sudden decrease due to leakage from the intestine was observed. All measurements were performed in triplicates.

2.7. Preparation of animal experiments

All animal experiments were performed at the Animal Research Laboratory of Kyungpook National University and approved by the Animal Review Committee of Kyungpook National University (2022-0036). All procedures were performed in accordance with the National Institute of Health's Guide for the Care and Use of Laboratory Animals. Forty normal male Sprague-Dawley rats (32 male rats, aged 6–8 weeks, body weight 200–250 g, Chungchengbuk-do, Korea) were used for intestinal anastomosis. All rats were housed, one per cage, in a temperature-controlled room (23 °C), fed a standard laboratory diet and tap water, and kept on a 12-h light/12-h dark cycle.

2.8. Animal models for the effectiveness evaluation of CHI-G/cHA double-layer patch

An AL model was developed using a method similar to that described in our previous study [17]. All operations were performed after sterilization and disinfection by a team of experienced clinical surgeons. General anesthesia was induced by isoflurane inhalation after a 24-h fast and the abdominal skin was shaved. Under sterile conditions using a

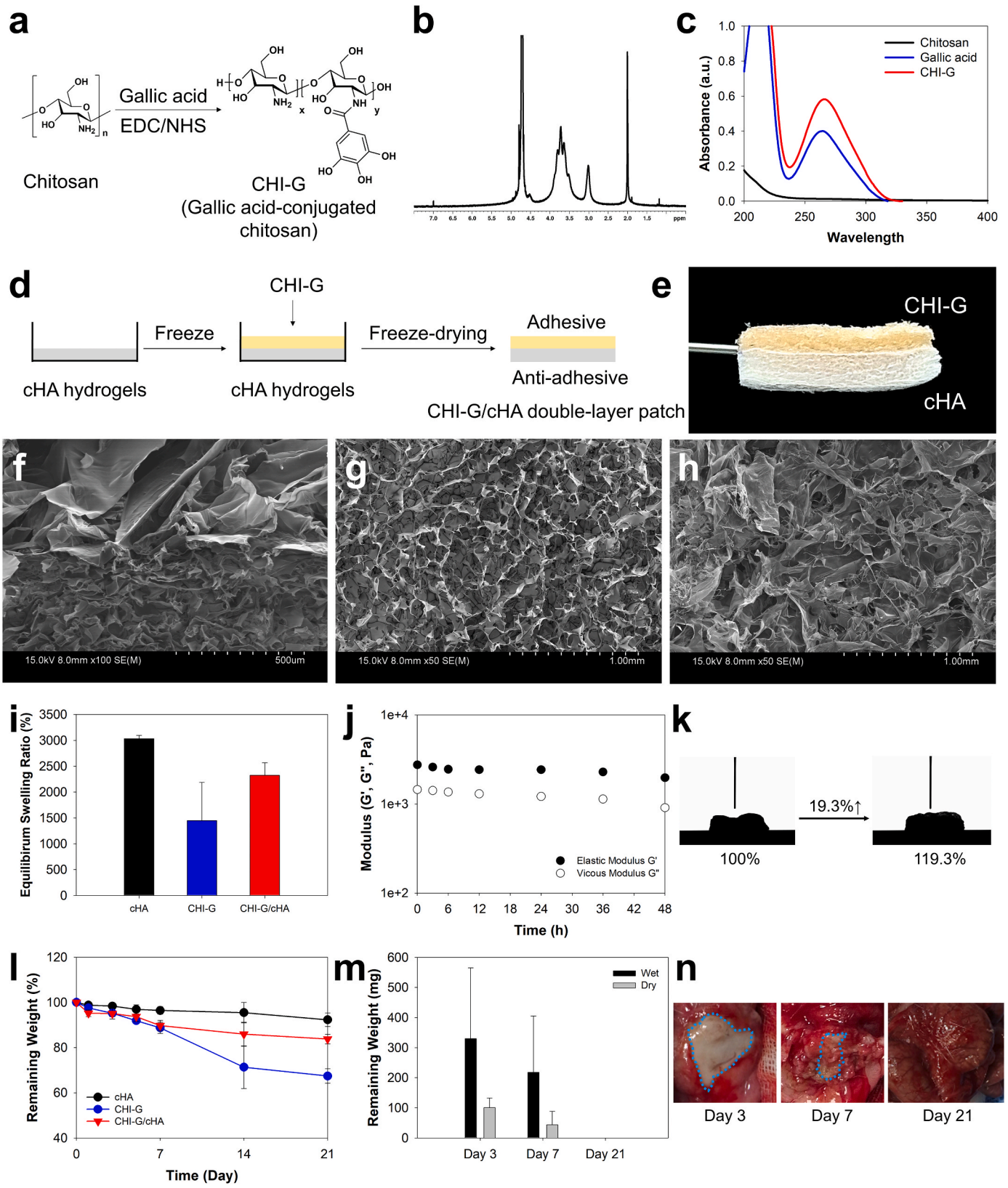

Fig. 2. a) Synthesis and chemical structures of CHI-G. b) ^{1}H NMR and c) UV–Vis spectra of CHI-G. d) Fabrications of CHI-G/cHA double-layer adhesives. HA hydrogels prepared using EDC (first) were frozen and CHI-G was poured onto the frozen HA hydrogels (second), and these were freeze-dried (third). e) Photographic images of CHI-G/cHA double-layer adhesives. f-h) SEM images of f) a cross-section (top: CHI-G and bottom: cHA) of CHI-G/cHA double-layer patches, g) inner surfaces of cHA, and h) inner surfaces of CHI-G. i) Equilibrium swelling ratios after 24-h incubation. j) Elastic (G') and viscous (G″) modulus changes in CHI-G alone as a function of time. k) Volume changes before and after PBS treatments measured by a water contact angle analyzer. l) *In vitro* and m) *in vivo* remaining weights of cHA, CHI-G, and CHI-G/cHA double-layer patches after predetermined time intervals. n) Photographic images of CHI-G/cHA double-layer patches-attached on anastomosis sites after 3, 7, and 21 days.

povidone-iodine scrub, a mid-abdominal incision was made to expose the peritoneal cavity and a linear enterotomy (1 cm long) was performed at the cecum. Subsequently, a loose anastomosis was performed using two 4-0 vicryl sutures.

Forty rats were randomly assigned to five groups (n = 8 per group) according to the material applied to the anastomosis site: 1) control (two-stitch only), 2) Mediclore™ (commercial anti-adhesive, CGBIO Ltd., Korea), 3) Neoveil™ (Commercial tissue-adhesive, Gunze Ltd., Japan), 4) CHI-G, and 5) CHI-G/cHA. Mediclore™ is a mixture of poloxamer, gelatin, and chitosan that is the commercially available anti-adhesive product. Neoveil™ is an absorbable reinforcement material prepared using polyglycolic acid (PGA). After all procedures were performed, the incisional abdominal cavity was closed with double layer using 3-0 vicryl continuous sutures for the fascia and 2-0 silk intermittent sutures for the skin. After the experimental rats awoke normally from anesthesia, they were fed a normal diet and observed individually in separate cages.

2.9. Assessment of adhesion scores

Half of the rats in each group were euthanized by inhalation after postoperative day 7 and the other half after postoperative day 21 using carbon dioxide inhalation. To determine the degree of adhesion, the abdomen was cut in a U-shape, and the degree of adhesion was scored according to the qualitative adhesion scoring system as follows. The adhesion score was evaluated based on three criteria: extent, type, and tenacity (total 10 points). Adhesion scores were evaluated according to the extent, type, and tenacity based on the macroscopic appearance of adhesions. Extent was 0 (no adhesion), 1 (1–25% of the peritoneal cavity involved), 2 (25–50% of the peritoneal cavity involved), 3 (51–75% of the peritoneal cavity involved), and 4 (76–100% of the peritoneal cavity involved); type was 0 (no adhesion), 1 (filmy), 2 (dense), and 3 (vascular); and tenacity was 0 (no adhesion), 1 (easily fall apart), 2 (requiring traction), 3 (requiring sharp dissection). Two independent clinical surgeons evaluated the adhesion scores in a blinded manner.

2.10. In vivo measurement of the anastomotic bursting pressure

After evaluating the adhesion score, en bloc excision of the ileocecal area, including the anastomosis, was performed. Subsequently, one side of the lumen of the specimen was ligated, and a pressure transducer catheter was inserted through the other side of the lumen and secured with ligation. Intraluminal pressure was measured by injecting air through the catheter using an infusion pump to gradually increase the luminal pressure of the specimen. The level at which a sudden pressure decline was observed was measured as the bursting pressure.

2.11. Hematologic assessment

For each group, 1.5 mL of preoperative and postoperative blood was placed in an SST tube (BD Vacutainer SST II Advance plus Blood Collection tubes) and 0.5 mL in an EDTA tube (BD Microtainer tube K2EDTA tubes). the SST tube was shaken around 5 times after collecting blood, kept at room temperature for 15 min, centrifuged at 3000 rpm for 10 min at 4 °C, and stored in a refrigerator (for long-term storage). The blood in the EDTA tube was shaken up and down approximately five times and refrigerated until required (storage X for more than one day).

2.12. Histological analysis

Histological analysis was conducted on paraffin-embedded 5-μm sections with peroxidase-conjugated affinity-isolated immunoglobulins. All intestinal segments that contained anastomosis were fixed in 10% neutral buffered formalin for 24 h and stained with H&E. The anastomosis was graded histologically in a blinded manner. Inflammatory cell infiltration, fibrosis of the anastomosis site, and fibrous adhesion between the anastomotic site and adjacent tissues (such as the abdominal wall and pericecal soft tissue) were graded from 0 to 4 as follows: 0 = no evidence, 1 = occasional evidence, 2 = light scattering, 3 = abundant evidence, and 4 = confluent cells or fibers. The fibrosis wall thickness (outer granulation rim of the leakage site) was determined as the median of four measurements per cecum cross-section. Three separate measurements were obtained for the fibrotic wall thickness in the granulation tissue at the leakage site, and the average values were calculated for the cecal wall.

3. Results and discussion

3.1. Synthesis and characterizations of CHI-G/cHA double-layer adhesives

To fabricate CHI-G/cHA double-layer adhesives, we first synthesized CHI-G. As shown in Fig. 2a, gallol moieties were introduced onto chitosan backbones by forming amide bonds between the amine groups of chitosan and the carboxylic acid groups of gallic acid. We performed ^{1}H NMR (D_2O) and UV–Vis spectroscopic studies on CHI-G to confirm the conjugation of gallic acid to chitosan. The aromatic ring protons of the gallol group in CHI-G were found between 7.0 and 7.5 ppm in the ^{1}H NMR spectra (Fig. 2b). In addition, an absorbance peak at 265 nm caused by gallic acid conjugation was observed in the UV–Vis spectra (Fig. 2c). The calculated degree of gallol substitution in the chitosan backbone was 6.0 ± 0.9% by comparing the absorbance at 265 nm of CHI-G and standard curves of gallic acid concentrations. CHI-G/cHA double-layer adhesives were prepared using a simple freeze-drying method. To prepare the cHA hydrogel patch layer, cHA hydrogels were first frozen in freeze-dried molds (Fig. 2d, first). The CHI-G solution (2 wt%) was poured onto the frozen cHA hydrogels (Fig. 2d, second), and both were lyophilized (Fig. 2d, third). Fig. 2e shows photographs of CHI-G/cHA double-layer adhesives. The slightly brown CHI-G layer, which may have been due to the color of gallic acid, was tangled with cHA layers in a disorderly manner. Cross-sectional scanning electron microscopic (SEM) images were obtained to confirm the morphology of CHI-G/cHA double-layer adhesives (Fig. 2f). Similar to the photographs, the two layers of CHI-G (top) and cHA (bottom) were integrated. We further obtained SEM images of cHA (Fig. 2g) and CHI-G (Fig. 2h). Relatively uniform and porous structures were observed in the cHA layer, whereas diverse uncontrollable structures were observed in the CHI-G layer. The interfaces between the CHI-G and cHA were further monitored with different magnifications. The morphologies were highly different between CHI-G and HA, but these were tightly combined in the interfaces probably due to electrostatic interactions with mechanical interlocking (Fig. S1). In addition, CHI-G and cHA layers were not separated by forceps even after treatments of water (Fig. S2).

Next, the equilibrium swelling ratio of the CHI-G/cHA double-layer adhesive was measured (Fig. 2i). After 24-h incubation, the swelling ratios were 3031 ± 65.3% for cHA, 1447 ± 738.7% for CHI-G, and 2325 ± 243.6% for CHI-G/cHA double-layer adhesives. Unexpectedly, we found that CHI-G patches alone were crosslinked by self-oxidation during patch preparation. UV–Vis spectra of CHI-G after re-lyophilization of patch preparations showed an overall upshift in absorbance at wavelengths >300 nm (Fig. S3). As previously reported, gallic acid-conjugated polymers were crosslinked in PBS (pH 7.4) solution by self-oxidation [39,40]. The elastic modulus (G') and viscous modulus (G″) did not change significantly as functions of incubation time (Fig. 2j), indicating that crosslinking of CHI-G occurred during the freeze-drying step. To monitor the volume expansion of CHI-G/cHA double-layer adhesives after water treatments, PBS solution (pH 7.4) was dropped into the adhesives. As shown in Fig. 2k, low volume expansion was observed after PBS treatments due to the porous sponge structures of double layer adhesives at the dry state. In addition, we monitored the remaining weights of cHA, CHI-G, and CHI-G/cHA double-layer adhesives in PBS (pH 7.4) solution. The remaining weights

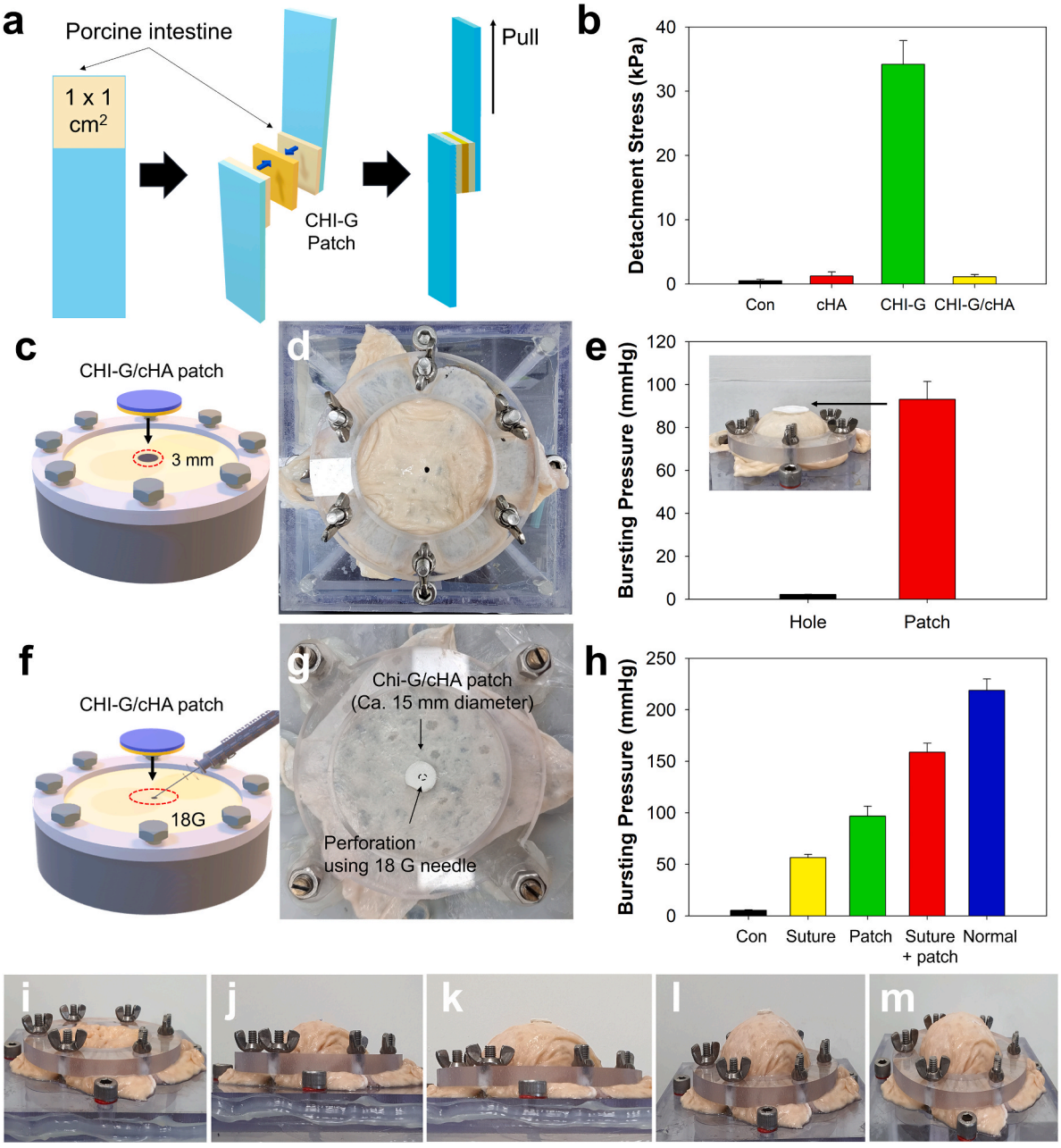

Fig. 3. a) Schematic illustrations of the measurement of tissue adhesive properties. b) Detachment stresses of cHA, CHI-G, and CHI-G/cHA double-layer patches after attachment on the porcine intestine. c) A schematic illustration and d) photographic image of bursting pressure measurements using a 3 mm biopsy punch. Porcine intestine was placed on the bursting pressure measurement devices and a hole with 3 mm diameter was made at the center of the intestine. After that, the CHI-G/cHA double-layer patch was attached to the hole. e) Detected bursting pressures after preparation of the hole and applying the patches over the hole, respectively. f) An illustration and g) a photo of bursting pressure measurements using an 18-gauge needle. The measurements were performed by a method similar to that described above. h) Bursting pressures after suturing, applying the CHI-G/cHA double-layer patch, after suturing with the CHI-G/cHA double-layer patch. (i–m) Photographic images of the intestine with perforation (i), after suturing (j), applying the CHI-G/cHA double-layer patch (k), after suturing with the CHI-G/cHA double-layer patch (l), and normal tissue without the perforation (m).

were 92.3 ± 2.9% for cHA, 67.4 ± 3.1% for CHI-G, and 83.7 ± 2.1% for CHI-G/cHA double-layer adhesives after 21 days (Fig. 2l). This might be due to the dissociation of the uncrosslinked CHI-G fractions of the double-layer adhesives in the PBS (pH 7.4) solution. We further monitored *in vivo* stabilities of double-layer adhesives at the anastomosis sites. CHI-G/cHA double-layer adhesives were attached to the anastomosis sites and monitored as a function of time (Fig. 2m and n). After 3 and 7 days, the adhesives were remained on the tissue. However, there was no adhesives after 21 days (Fig. 2n). The remaining weights of CHI-G/cHA double-layer adhesives in wet conditions were 330.2 ± 235.2 mg after 3 days, 218.3 ± 187.2 mg after 7 days, and 0 mg after 21 days (Fig. 2m). In addition, the remaining weights of these adhesives after freeze-drying were 100.5 ± 32.0 mg after 3 days, 43.8 ± 44.3 mg after 7 days, and 0 mg after 21 days. In general, most leakages after intestinal anastomosis occur within the first week [41,42]. It was noteworthy that the adhesives can be act as sealing materials during the healing steps of anastomotic defects and absorbed at the longer time.

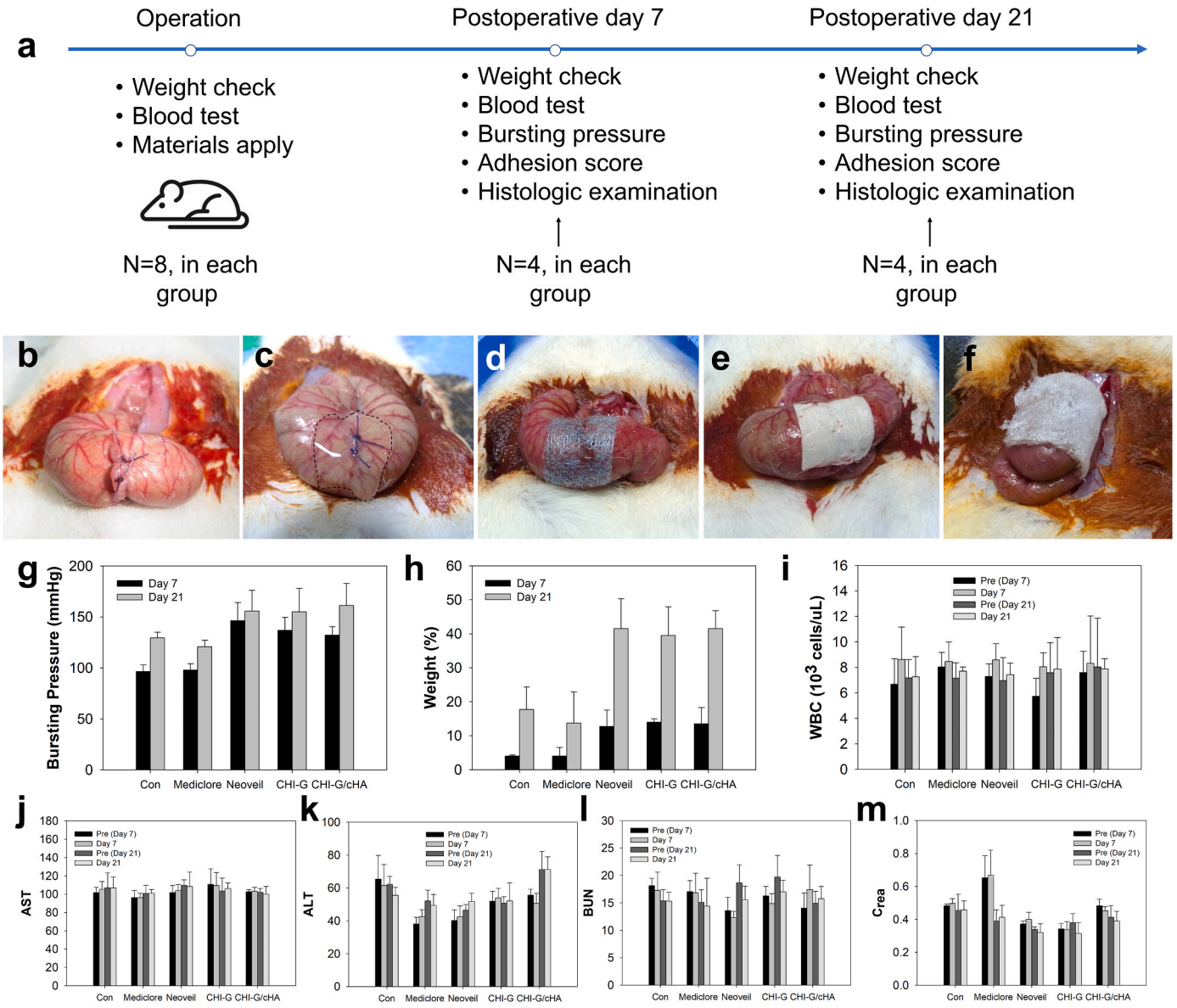

Fig. 4. a) Surgical procedures for AL. (b–f) Photographs of CHI-G/cHA double-layer patches on intestinal anastomosis. The animal model of AL was created by incising the cecum approximately 2 cm and suturing it with two stitches. b) Control group: two-stitch sutures only and other group; c) Mediclore™, d) Neoveil™, e) CHI-G, and f) CHI-G/cHA were applied to the anastomotic site, respectively. g) Bursting pressure, h) weight, i) WBC, j) AST, k) ALT, l) BUN, m) Crea changes in each group on postoperative days 7 and 21.

3.2. Adhesion forces of CHI-G/cHA double-layer adhesives

The adhesion forces of the CHI-G/cHA double-layer adhesive attached to the intestine were measured (Fig. 3a). As shown in Fig. 3b, the detachment stress of CHI-G patches alone was 34 ± 3.7 kPa, which was considerably higher than those of the control and cHA patches. CHI-G/cHA double-layer adhesives showed 1.1 ± 0.3 kPa of detachment stress, which was significantly lower than that with the CHI-G patches due to the cHA layers. In addition, we measured the bursting pressure of the porcine intestine after sealing the perforation sites with the CHI-G/cHA double-layer adhesive. Bursting pressure is one of the most reliable indicators of the degree of anastomotic sealing; therefore, this pressure was measured in a manner similar to that in previous reports [43–46]. The bursting pressures were firstly measured in accordance with ASTM F2392-04 test methods. After preparations of a hole with 3 mm diameter, the CHI-G/cHA double-layer adhesives (15 mm diameter) were applied over the hole (Fig. 3c and d). After applying the CHI-G/cHA double-layer adhesives to the hole, pressure was monitored with an air supply into the chamber covered with the porcine intestine. The measured bursting pressures of intestine with a 3 mm hole was 2.2 ± 0.1 mmHg, but the bursting pressures were remarkably increased to 93.1 ± 8.3 mmHg (Fig. 3e). To closely test the bursting pressures in clinical settings, we prepared a perforated porcine intestine using 18-gauge needles (Fig. 3f and g). As shown in Fig. 3h, the bursting pressure in the untreated control group was 218.8 ± 11.1 mmHg. After supplying air into the intestine, there was no inflation due to the perforation (Fig. 3i and Fig. S2a). After sealing the perforation site with suture, the bursting pressure increased to 56.4 ± 3.1 mmHg, which was far lower than that of the normal tissue without perforation. Reduction in the bursting pressure after suturing might be due to suture holes (Fig. 3j and Fig. S2b). In case of the CHI-G/cHA double-layer adhesive group, bursting pressure was 96.7 ± 9.6 mmHg, which was 1.75 times higher than that of suturing groups. In addition, significant intestinal inflation was observed (Fig. 3k and Fig. S2c). In addition, the bursting pressure further increased to 158.7 ± 8.8 mmHg when we applied the CHI-G/cHA double-layer adhesive after suturing (Fig. 3l). The bursting

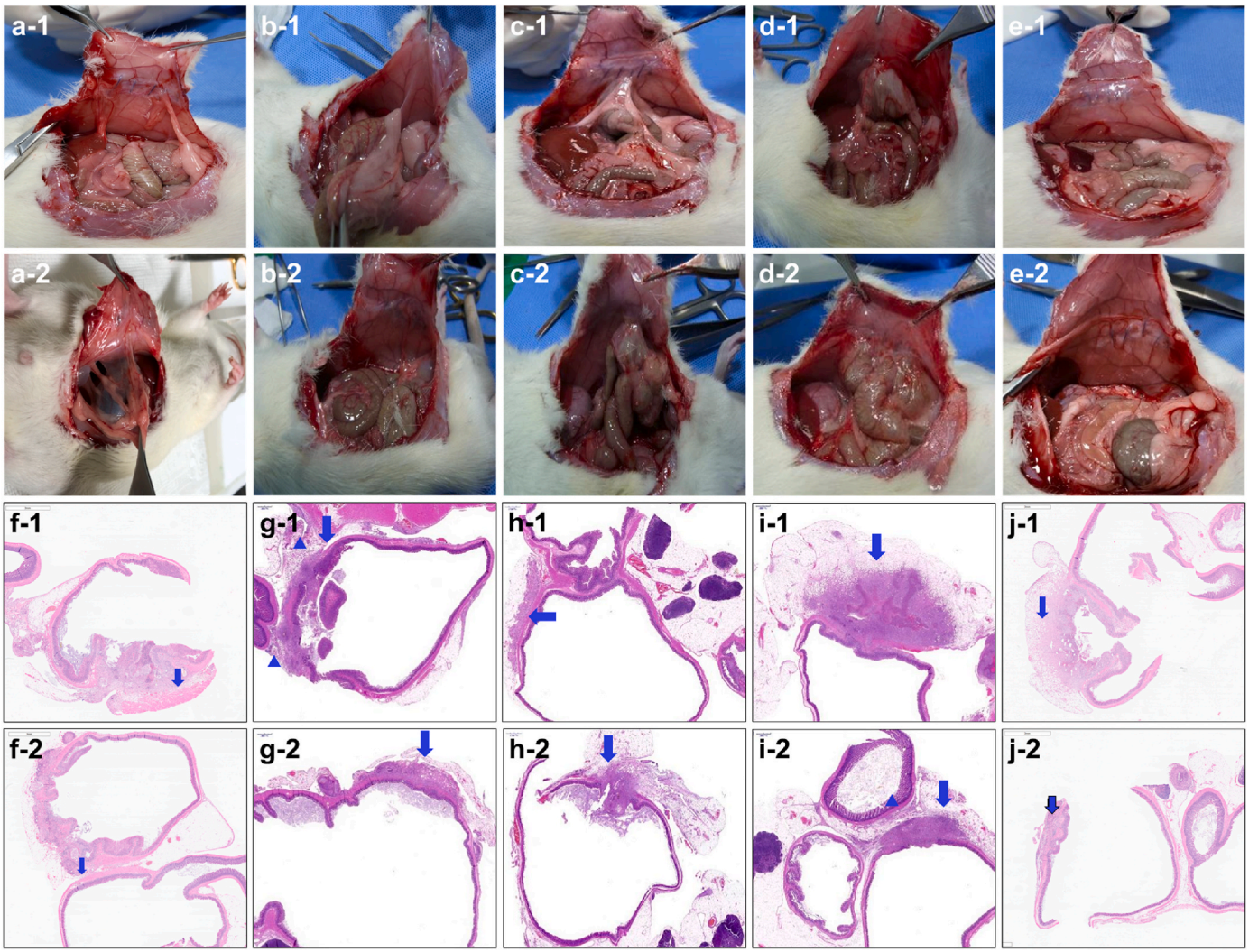

Fig. 5. (a–e) Gross finding of the extent of adhesion on postoperative day 7 and 21. a) control, b) Mediclore™, c) Neoveil™, d) CHIi-G, and e) CHI-G/cHA. (f–j) Histological findings on H/E images of the anastomosis on postoperative day 7 and 21. f) control, g) Mediclore™, h) Neoveil™, i) CHII-G, and j) CHI-G/cHA. Number 1 indicate the image acquired on postoperative day 7 and number 2 indicates the image acquired on postoperative day 21.

pressures and intestine inflation were comparable with those of normal tissues (Fig. 3m). It is noteworthy that the CHI-G/cHA double-layer adhesives are usefully exploited as intestinal anastomotic supporting materials, considering the intestinal anastomosis surgical procedures with sutures or staplers.

3.3. Effects of CHI-G/cHA double-layer patches on intestinal anastomosis

An animal model of AL was prepared using a method similar to that described in a previous study [17], as shown in Fig. 4a. In brief, a mid-abdominal incision of approximately 4 cm in length was made for peritoneal cavity exposure, and linear enterotomy (1 cm in length) was performed at the cecum. Subsequently, a loose anastomosis was performed using two of the 4-0 vicryl sutures. The rats were then randomly assigned to five groups according to the material applied to the anastomosis site as follows: 1) control (two-stitch only), 2) Mediclore™, 3) Neoveil™, 4) CHI-G, and 5) CHI-G/cHA (Fig. 4b–f). After performing all procedures, the incisional abdominal cavity was closed. After the experimental rats awoke normally from anesthesia, they were fed a normal diet and observed individually in separate cages. Half of each group was euthanized by inhalation after 7 days (n = 4 in each group), and the other half was euthanized after 21 days (n = 4 in each group) using carbon dioxide.

We observed that the luminal bursting pressure prevented AL (Fig. 4g). On postoperative day 7, the bursting pressure was significantly higher in the three groups that received tissue adhesive to the anastomotic site materials than in the control and Mediclore™ groups. The mean bursting pressure of the CHI-G/cHA group was 1.37 times higher than that of the control group, which was statistically significant (96.4 ± 6.5 vs. 132.3 ± 8.3 mmHg, $p < 0.05$). There was no significant difference in the mean bursting pressure between the tissue adhesive groups. The mean bursting pressure of the Mediclore™ group was significantly lower than that of the other tissue adhesives-treated groups, but there was no difference compared with the control group. On postoperative day 21, the mean bursting pressure increased in all groups; however, the results were similar to those obtained on postoperative day 7. The mean bursting pressure of the CHI-G/cHA group (161.1 ± 21.6 mmHg) was higher than those of the control (129.4 ± 5.7 mmHg, $p < 0.05$) and Mediclore™ groups (120.8 ± 5.2 mmHg, $p < 0.05$). The body weights of each subject were measured before and after surgery in each group on the day of the operation and on postoperative days 7 and 21. Although there was a trend of weight gain over time after surgery compared with that before surgery in all groups, the weight gain in the group using tissue adhesives was more significant than that in the control and Mediclore™ groups (Fig. 4h).

To investigate the inflammatory response of the material applied to

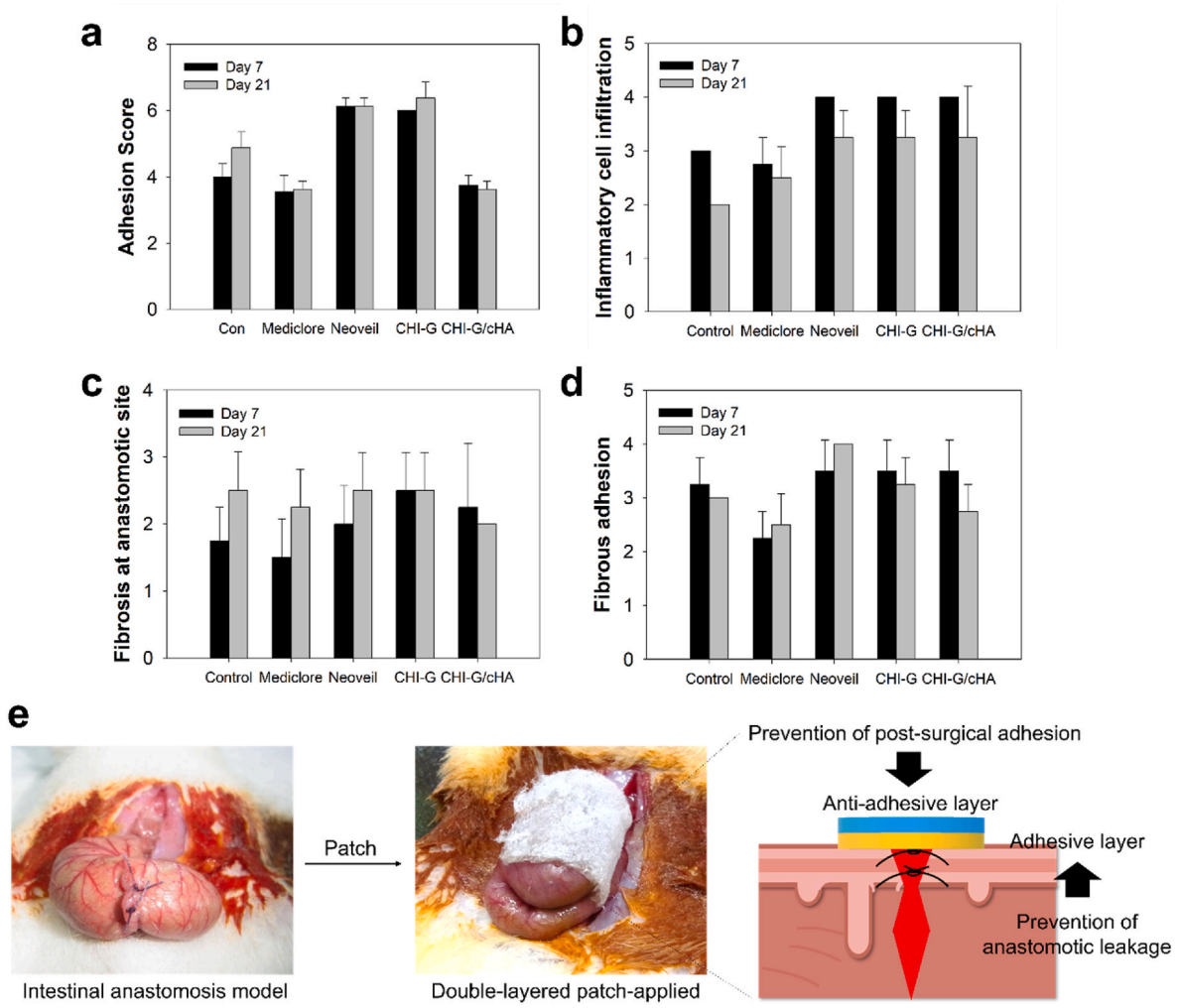

Fig. 6. a) adhesion score from gross findings scored by surgeons. (b–d) Scores of histologic findings scored by a pathologist, b) inflammatory cell infiltration, c) fibrosis of the anastomotic site, and d) fibrous adhesion between the anastomotic site and adjacent tissue. e) Schematic representatives of CHI-G/cHA double layer patches for preventing anastomotic leakage and reducing post-surgical adhesion.

the animals, the white blood cell (WBC) count was examined before surgery and on the day of euthanasia (postoperative days 7 and 21). The WBC count was within the normal range in all groups preoperatively, and on postoperative day 7, it tended to increase compared to that before surgery, but there was no significant difference between the groups. On postoperative day 21, the WBC count tended to decrease compared with that on postoperative day 7 in all groups (Fig. 4i). Although blood test results differed depending on the subject or time of blood sample collection, both liver and kidney function tests were within the normal range. There was no specific pattern in the measurement values according to the group or time of blood sample collection (Fig. 4j–m). Based on these results, CHI-G/cHA double-layer materials may not cause hepatotoxicity or renal toxicity when applied *in vivo*.

3.4. Anti-adhesive properties and histopathologic examinations

Adhesion scores were evaluated according to qualitative adhesion scoring, as previously reported [17]. To determine the degree of adhesion, the abdomen was cut into a U-shape on the day of euthanization, and the degree of adhesion was scored according to the qualitative adhesion scoring system [14]. Two independent clinical surgeons evaluated the adhesion score in a blinded manner using photographs and videos. The photograph depicts the extent of adhesion between the groups on postoperative day 7 and 21(Fig. 5a–e). In general, both the Mediclore™ group and the Chi-G/cHA group exhibited a tendency to experience fewer adhesions both 7 and 21 days after surgery. In histological analysis, moderate acute inflammation, and moderate fibrosis with adhesion to the peritoneum were observed in control (Fig. 5f, arrow). Mediclore™ groups showed mild acute inflammation and mild fibrosis (arrow) with focal adhesion to adjacent organ (arrowhead) on postoperative day 7, but adhesion was dissolved on postoperative day 21 (Fig. 5g). In case of the Neoveil™ groups, moderate chronic inflammation, and moderate fibrosis (arrow) were found (Fig. 5h). The CHI-G adhesive groups showed abscess formation on postoperative day 7 (arrow), and moderate chronic inflammation and moderate fibrosis (arrowhead) with adhesion to the small intestine wall (arrowhead) on postoperative day 21 (Fig. 5i). Pericolic tissues of CHI-G/cHA groups showed moderate acute inflammation and fibrosis, but no adhesion to the adjacent organ (Fig. 5j). The process of intestinal wound healing is generally similar to that of other parts of the body, typically advancing through the stages of inflammation, proliferation, and maturation [47]. If the inflammatory phase persists for an extended period, it can hinder wound healing and increase the risk of anastomotic disruption. In theory, the use of tissue adhesives during the inflammatory phase could potentially enhance the strength of the anastomosis by promoting fibroblast proliferation [48,49]. However, fibrosis caused by the excessive proliferation of fibroblasts and chronic inflammation can cause

unintended adhesions [50,51]. Based on this, we believe that the observed increase in burst pressure in the group using tissue adhesive in our results is likely due to an increase in inflammation and fibrosis, which contribute to the strengthening of the anastomosis site. On the other hand, there was a tendency for adhesions to further increase also observed in the group that used tissue adhesives.

The mean adhesion scores on postoperative day 7 were lower in the Mediclore™ and CHI-G/cHA groups than in the Neoveil™ and CHI-G groups. However, no differences were observed between the control, Mediclore™, and CHI-G/cHA groups. On postoperative day 21, the mean adhesion scores of the Mediclore™ and CHI-G/cHA groups were significantly lower than those of the control, Neoveil™, and CHI-G groups. However, no difference was observed between the Mediclore™ and CHI-G/cHA groups (Fig. 6a). Our results regarding the adhesion score are similar to those of previous reports, which showed that Mediclore™ and HA act as barriers between organs, preventing adhesion by inhibiting the proliferation of fibroblasts [52,53]. The inflammatory cell infiltration score was higher on postoperative day 7 than on postoperative day 21 in all groups. In particular, the mean of the inflammatory cell infiltration scores in groups of the applied tissue adhesive materials was higher than those of the control and Mediclore™ groups (Fig. 6b). In contrast, the degree of fibrosis in the anastomotic site tended to be higher on postoperative day 21 than on postoperative day 7, except in the CHI-G/cHA group (Fig. 6c and d). Based on these results, we expect that the double-layer patch, CHI-G/cHA, will show an anti-adhesive effect similar to that of Mediclore™. In addition, unintended adhesions can be prevented even when using tissue adhesive materials.

4. Conclusions

In summary, adhesive/anti-adhesive double-layer patches using CHI-G as adhesive materials and crosslinked HA as anti-adhesive materials were developed. Adhesive layers of the double-layer patches showed excellent adhesion to intestinal tissue surfaces. Double-layer adhesives were effective in anastomosis by sealing the perforation sites. In addition, the patches reduced postsurgical adhesion owing to the crosslinked HA. Thus, we expect that adhesive/anti-adhesive double-layer patches have enormous potential as sealing materials for anastomotic sites with reduced post-surgical adhesion, particularly for intestinal anastomosis after colorectal surgery.

Credit author statement

Sung Il Kang: Conceptualization, Methodology, Validation, Formal analysis, Investigation, Data curation, Writing – original draft, Writing – review & editing, Visualization. Hyun Ho Shin: Methodology, Validation, Formal analysis, Investigation, Da Han Hyun: Methodology, Validation, Formal analysis, Investigation, Ghilsuk Yoon: Methodology, Validation, Formal analysis, Investigation, Jun Seok Park: Supervision, Funding acquisition, Conceptualization, Methodology, Validation, Ji Hyun Ryu: Supervision, Funding acquisition, Conceptualization, Methodology, Validation, Formal analysis, Investigation, Data curation, Writing – original draft, Writing – review & editing.

Declaration of competing interest

The authors declare that there is no conflict of interest.

Data availability

Data will be made available on request.

Acknowledgments

This research was supported by the National Research Foundation of Korea (NRF) grant funded by the Korean government (MSIT) (2022R1A4A1031259, JHR) and the Korean Fund for Regenerative Medicine (KFRM) grant funded by the Korea government (Ministry of Science and ICT and Ministry of Health & Welfare) (22A0103L1, JHR). This work was partially supported by the National Research Foundation of Korea (NRF) grant funded by the Korea government (MSIT) (2020R1A2C1010750, JSP).

Appendix A. Supplementary data

Supplementary data to this article can be found online at https://doi.org/10.1016/j.mtbio.2023.100806.

References

[1] M. Degiuli, U. Elmore, R. De Luca, P. De Nardi, M. Tomatis, A. Biondi, R. Persiani, L. Solaini, G. Rizzo, D. Soriero, D. Cianflocca, M. Milone, G. Turri, D. Rega, P. Delrio, C. Pedrazzani, G.D. De Palma, F. Borghi, S. Scabini, C. Coco, D. Cavaliere, M. Simone, R. Rosati, R. Reddavid, G. collaborators, From the Italian society of surgical oncology colorectal cancer network collaborative, risk factors for anastomotic leakage after anterior resection for rectal cancer (RALAR study): a nationwide retrospective study of the Italian society of surgical oncology colorectal cancer network collaborative group, Colorectal Dis. 24 (3) (2022) 264–276, https://doi.org/10.1111/codi.15997.

[2] M. Jessen, M. Nerstrom, T.E. Wilbek, S. Roepstorff, M.S. Rasmussen, P.M. Krarup, Risk factors for clinical anastomotic leakage after right hemicolectomy, Int. J. Colorectal Dis. 31 (9) (2016) 1619–1624, https://doi.org/10.1007/s00384-016-2623-5.

[3] C.Y. Kang, W.J. Halabi, O.O. Chaudhry, V. Nguyen, A. Pigazzi, J.C. Carmichael, S. Mills, M.J. Stamos, Risk factors for anastomotic leakage after anterior resection for rectal cancer, JAMA Surg 148 (1) (2013) 65–71, https://doi.org/10.1001/2013.jamasurg.2.

[4] W. Zhang, Z. Lou, Q. Liu, R. Meng, H. Gong, L. Hao, P. Liu, G. Sun, J. Ma, W. Zhang, Multicenter analysis of risk factors for anastomotic leakage after middle and low rectal cancer resection without diverting stoma: a retrospective study of 319 consecutive patients, Int. J. Colorectal Dis. 32 (10) (2017) 1431–1437, https://doi.org/10.1007/s00384-017-2875-8.

[5] S.I. Kang, S. Kim, J.H. Kim, Two-year follow-up results of the use of a fecal diverting device as a substitute for a defunctioning stoma, Int. J. Colorectal Dis. 37 (4) (2022) 835–841, https://doi.org/10.1007/s00384-022-04117-7.

[6] J.W. Bosmans, A.C. Jongen, N.D. Bouvy, J.P. Derikx, Colorectal anastomotic healing: why the biological processes that lead to anastomotic leakage should be revealed prior to conducting intervention studies, BMC Gastroenterol. 15 (2015) 180, https://doi.org/10.1186/s12876-015-0410-3.

[7] Z.A. Murrell, M.J. Stamos, Reoperation for anastomotic failure, Clin. Colon Rectal Surg. 19 (4) (2006) 213–216, https://doi.org/10.1055/s-2006-956442.

[8] G. Nandakumar, S.L. Stein, F. Michelassi, Anastomoses of the lower gastrointestinal trac, Nat. Rev. Gastroenterol. Hepatol. 6 (12) (2009) 709–716, https://doi.org/10.1038/nrgastro.2009.185.

[9] A. Akgun, S. Kuru, C. Uraldi, O. Tekin, B. Karip, T. Tug, A.U. Ongoren, Early effects of fibrin sealant on colonic anastomosis in rats: an experimental and case-control study, Tech. Coloproctol. 10 (3) (2006) 208–214, https://doi.org/10.1007/s10151-006-0281-2.

[10] Z. Wu, G.S. Boersema, L.F. Kroese, D. Taha, S. Vennix, Y.M. Bastiaansen-Jenniskens, K.H. Lam, G.J. Kleinrensink, J. Jeekel, M. Peppelenbosch, J.F. Lange, Reducing colorectal anastomotic leakage with tissue adhesive in experimental inflammatory bowel disease, Inflamm. Bowel Dis. 21 (5) (2015) 1038–1046, https://doi.org/10.1097/MIB.0000000000000336.

[11] Z. Wu, K.A. Vakalopoulos, L.F. Kroese, G.S. Boersema, G.J. Kleinrensink, J. Jeekel, J.F. Lange, Reducing anastomotic leakage by reinforcement of colorectal anastomosis with cyanoacrylate glue, Eur. Surg. Res. 50 (3–4) (2013) 255–261, https://doi.org/10.1159/000350383.

[12] J. Paral, Z. Subrt, P. Lochman, L. Klein, D. Hadzi-Nikolov, Z. Turek, M. Vejbera, Suture-free anastomosis of the colon. Experimental comparison of two cyanoacrylate adhesives, J. Gastrointest. Surg. 15 (3) (2011) 451–459, https://doi.org/10.1007/s11605-010-1370-0.

[13] Z. Wu, G.S. Boersema, K.A. Vakalopoulos, F. Daams, C.L. Sparreboom, G. J. Kleinrensink, J. Jeekel, J.F. Lange, Critical analysis of cyanoacrylate in intestinal and colorectal anastomosis, J. Biomed. Mater. Res. Part B Appl. Biomater. 102 (3) (2014) 635–642, https://doi.org/10.1002/jbm.b.33039.

[14] K.A. Vakalopoulos, Z. Wu, L. Kroese, G.J. Kleinrensink, J. Jeekel, R. Vendamme, D. Dodou, J.F. Lange, Mechanical strength and rheological properties of tissue adhesives with regard to colorectal anastomosis: an ex vivo study, Ann. Surg. 261 (2) (2015) 323–331, https://doi.org/10.1097/SLA.0000000000000599.

[15] K.B. Bae, S.H. Kim, S.J. Jung, K.H. Hong, Cyanoacrylate for colonic anastomosis; is it safe? Int. J. Colorectal Dis. 25 (5) (2010) 601–606, https://doi.org/10.1007/s00384-009-0872-2.

[16] S.C. Woodward, J.B. Herrmann, J.L. Cameron, G. Brandes, E.J. Pulaski, F. Leonard, Histotoxicity of cyanoacrylate tissue adhesive in the rat, Ann. Surg. 162 (1) (1965) 113–122, https://doi.org/10.1097/00000658-196507000-00017.

[17] S. Girgin, H. Ozturk, E. Gedik, V. Akpolat, E. Kale, H. Ozturk, Effect of a 50-Hz Sinusoidal electromagnetic field on the integrity of experimental colonic anastomoses covered with fibrin glue, Adv. Clin. Exp. Med. 18 (1) (2009) 13–18.

[18] L.C. Capitan Morales, E. Rodriguez Nunez, S. Morales Conde, F. Sanchez Ganfornina, F.D. Del Rio Lafuente, E. Cabot Ostos, J.M. Ortega Bevia, J. Loscertales Abril, J. Cantillana Martinez, Experimental study of sutureless colorectal anastomosis, Hepato-Gastroenterology 47 (35) (2000) 1284–1290.

[19] K. Hirai, Y. Tabata, S. Hasegawa, Y. Sakai, Enhanced intestinal anastomotic healing with gelatin hydrogel incorporating basic fibroblast growth factor, J. Tissue Eng. Regen. Med. 10 (10) (2016) E433–E442, https://doi.org/10.1002/term.1835.

[20] G. Joo, T. Sultana, S. Rahaman, S.H. Bae, H.I. Jung, B.T. Lee, Polycaprolactone-gelatin membrane as a sealant biomaterial efficiently prevents postoperative anastomotic leakage with promoting tissue repair, J. Biomater. Sci. Polym. Ed. 32 (12) (2021) 1530–1547, https://doi.org/10.1080/09205063.2021.1917107.

[21] T. Vuocolo, R. Haddad, G.A. Edwards, R.E. Lyons, N.E. Liyou, J.A. Werkmeister, J. A. Ramshaw, C.M. Elvin, A highly elastic and adhesive gelatin tissue sealant for gastrointestinal surgery and colon anastomosis, J. Gastrointest. Surg. 16 (4) (2012) 744–752, https://doi.org/10.1007/s11605-011-1771-8.

[22] T. Nordentoft, Sealing of gastrointestinal anastomoses with fibrin glue coated collagen patch, Dan. Med. J. 62 (5) (2015) B5081.

[23] T. Nordentoft, K. Holte, Preventing clinical leakage of colonic anastomoses with a fibrin-coated collagen patch sealing-an experimental study, Arch. Clin. Exp. Surg. 3 (2013) 201–206, https://doi.org/10.5455/aces.20130321071651.

[24] M.H. Schreinemacher, J.G. Bloemen, S.J. Van der Heijden, M.J. Gijbels, C. H. Dejong, N.D. Bouvy, Collagen fleeces do not improve colonic anastomotic strength but increase bowel obstructions in an experimental rat model, Int. J. Colorectal Dis. 26 (2011) 729–735, https://doi.org/10.1007/s00384-011-1158-z.

[25] Y. Altinel, S.S. Chung, G. Okay, N. Ugras, A.F. Isik, E. Ozturk, H. Ozguc, Effect of chitosan coating on surgical sutures to strengthen the colonic anastomosis, Ulus. Travma Acil Cerrahi Derg. 24 (5) (2018) 405–411, https://doi.org/10.5505/tjtes.2018.59280.

[26] B. Citgez, A.N. Cengiz, I. Akgun, M. Uludag, G. Yetkin, N. Bahat, O. Ozcan, N. Polat, A. Akcakaya, O. Karatepe, Effects of chitosan on healing and strength of colonic anastomosis in rats, Acta Cir. Bras. 27 (10) (2012) 707–712, https://doi.org/10.1590/s0102-86502012001000007.

[27] Y. Zheng, A.F. Pierce, W.L. Wagner, H.A. Khalil, Z. Chen, C. Funaya, M. Ackermann, S.J. Mentzer, Biomaterial-assisted anastomotic healing: serosal adhesion of pectin films, Polymers 13 (16) (2021) 2811, https://doi.org/10.3390/polym13162811.

[28] A.H.C. Anthis, X.Q. Hu, M.T. Matter, A.L. Neuer, K.C. Wei, A.A. Schlegel, F.H. L. Starsich, I.K. Herrmann, Chemically stable, strongly adhesive sealant patch for intestinal anastomotic leakage prevention, Adv. Funct. Mater. 31 (16) (2021), 2007099, https://doi.org/10.1002/adfm.202007099.

[29] J.H. Ryu, H. Kim, K. Kim, G. Yoon, Y. Wang, G.S. Choi, H. Lee, J.S. Park, Multipurpose intraperitoneal adhesive patches, Adv. Funct. Mater. 29 (29) (2019), 1900495, https://doi.org/10.1002/adfm.201900495.

[30] R.P. Ten Broek, Y. Issa, E.J. Van Santbrink, N.D. Bouvy, R.F. Kruitwagen, J. Jeekel, E.A. Bakkum, M.M. Rovers, H. Van Goor, Burden of adhesions in abdominal and pelvic surgery: systematic review and met-analysis, BMJ 3 (2013) 347, https://doi.org/10.1136/bmj.f5588, f5588.

[31] W.S. Kang, Y.C. Park, Y.G. Jo, J.C. Kim, Early postoperative small bowel obstruction after laparotomy for trauma: incidence and risk factors, Ann. Surg. Treat. Res. 94 (2) (2018) 94–101, https://doi.org/10.4174/astr.2018.94.2.94.

[32] H. Yao, M. Wu, L. Lin, Z. Wu, M. Bae, S. Park, S. Wang, W. Zhang, J. Gao, D. Wang, Y. Piao, Design strategies for adhesive hydrogels with natural antibacterial agents as wound dressings: status and trends, Mater. Today Bio 16 (2022), 100429, https://doi.org/10.1016/j.mtbio.2022.100429.

[33] Z. Aliakbar Ahovan, Z. Esmaeili, B.S. Eftekhari, S. Khosravimelal, M. Alehosseini, G. Orive, A. Dolatshahi-Pirouz, N. Pal Singh Chauhan, P.A. Janmey, A. Hashemi, S. C. Kundu, M. Gholipourmalekabadi, Antibacterial smart hydrogels: new hope for infectious wound management, Mater. Today Bio 17 (2022), 100499, https://doi.org/10.1016/j.mtbio.2022.100499.

[34] Y. He, Q. Li, P. Chen, Q. Duan, J. Zhan, X. Cai, L. Wang, H. Hou, X. Qiu, A smart adhesive Janus hydrogel for non-invasive cardiac repair and tissue adhesion prevention, Nat. Commun. 13 (1) (2022) 7666, https://doi.org/10.1038/s41467-022-35437-5.

[35] P. Qi, Y.G. Zheng, S. Ohta, N. Kokudo, K. Hasegawa, T. Ito, In situ fabrication of double-layered hydrogels via spray processes to prevent postoperative peritoneal adhesion, ACS Biomater. Sci. Eng. 5 (9) 4790-4798. DOI: https://doi.org/10.1021/acsbiomaterials.9b00791..

[36] H. Wang, X. Yi, T. Liu, J. Liu, Q. Wu, Y. Ding, L. Zhu, Q. Wang, An integrally formed janus hydrogel for robust wet-tissue adhesive and anti-postoperative adhesion, Adv. Mater. (2023), 2300364, https://doi.org/10.1002/adma.202300394.

[37] W. Peng, C. Liu, Y. Lai, Y. Wang, P. Liu, J. Shen, An adhesive/anti-adhesive janus tissue patch for efficient closure of bleeding tissue with inhibited postoperative adhesion, Adv. Sci. (2023), 2301427, https://doi.org/10.1002/advs.202301427.

[38] W. Yang, C. Xuan, X. Liu, Q. Zhang, K. Wu, L. Bian, X. Shi, A sandwiched patch toward leakage-free and anti-postoperative tissue adhesion sealing of intestinal injuries, Bioact. Mater. 24 (2023) 112–123, https://doi.org/10.1016/j.bioactmat.2022.12.003.

[39] J.S. Lee, J.H. Cho, S. An, J. Shin, S. Choi, E.J. Jeon, S.W. Cho, In situ self-cross-linkable, long-term stable hyaluronic acid filler by gallol autoxidation for tissue augmentation and wrinkle correction, Chem. Mater. 31 (23) (2019) 9614–9624, https://doi.org/10.1021/acs.chemmater.9b02802.

[40] Q.L. Yang, L.L. Tang, C.C. Guo, F. Deng, H. Wu, L.H. Chen, L.L. Huang, P. Lu, C. C. Ding, Y.H. Ni, M. Zhang, A bioinspired gallol-functionalized collagen as wet-tissue adhesive for biomedical applications, Chem. Eng. J. 417 (2021), 127962, https://doi.org/10.1016/j.cej.2020.127962.

[41] R.B. Morgan, B.D. Shogan, The science of anastomotic healing. The science of anastomotic healing, Semin. Colon Rectal Surg. (2022), 100879, https://doi.org/10.1016/j.scrs.2022.100879.

[42] S.K. Thompson, E.Y. Chang, B.A. Jobe, Clinical review: healing in gastrointestinal anastomoses, part I, Microsurgery 26 (3) (2006) 131–136, https://doi.org/10.1002/micr.20197.

[43] A.B. Costales, D. Patil, A. Mulya, J.P. Kirwan, C.M. Michener, 2-Octylcyanoacrylate for the prevention of anastomotic leak, J. Surg. Res. 226 (2018) 166–172, https://doi.org/10.1016/j.jss.2018.01.026.

[44] Y. Li, Y. Bao, T. Jiang, L. Tan, Y. Gao, J. Li, Effect of the combination of fibrin glue and growth hormone on incomplete intestinal anastomoses in a rat model of intra-abdominal sepsis, J. Surg. Res. 131 (1) (2006) 111–117, https://doi.org/10.1016/j.jss.2005.09.013.

[45] P. Senthil-Kumar, T. Ni, M.A. Randolph, G.C. Velmahos, I.E. Kochevar, R. W. Redmond, A light-activated amnion wrap strengthens colonic anastomosis and reduces peri-anastomotic adhesions, Laser Surg. Med. 48 (5) (2016) 530–537, https://doi.org/10.1002/lsm.22507.

[46] R.J. Verhage, A. Ruiz, A. Verheem, R. Goldschmeding, I.H. Borel Rinkes, R. van Hillegersberg, Fibrin-thrombin coated sealant increases strength of esophagogastric anastomoses in a rat model, J. Surg. Res. 176 (2) (2012) e57–e63, https://doi.org/10.1016/j.jss.2011.12.028.

[47] K.M. Mullen, P.J. Regier, G.W. Ellison, L. Londoño, A review of normal intestinal healing, intestinal anastomosis, and the pathophysiology and treatment of intestinal dehiscence in foreign body obstructions in dogs, Top. Companion Anim. Med. 41 (2020), 100457, https://doi.org/10.1016/j.tcam.2020.100457.

[48] C.M. DePompeo, L. Bond, Y.E. George, M.J. Mezzles, J.D. Brourman, J.C. Chandler, S.M. Murphy, D.R. Mason, Intra-abdominal complications following intestinal anastomoses by suture and staple techniques in dogs, J. Am. Vet. Med. Assoc. 253 (4) (2018) 437–443, https://doi.org/10.2460/javma.253.4.437.

[49] G.H. Ballantyne, J.B. Burke, G. Rogers, E.G. Lampert, J. Boccia, Accelerated wound healing with stapled enteric suture lines. an experimental study comparing traditional sewing techniques and a stapling device, Ann. Surg. 201 (3) (1985) 360–364, https://doi.org/10.1097/00000658-198503000-00019.

[50] F.O. The, R.J. Bennink, W.M. Ankum, M.R. Buist, O.R.C. Busch, D.J. Gouma, S. van der Heide, R.M. van den Wijngaard, W.J. de Jonge, G.E. Boeckxstaens, Intestinal handling-induced mast cell activation and inflammation in human postoperative ileus, Gut 57 (1) (2008) 33–40, https://doi.org/10.1136/gut.2007.120238.

[51] P. Ghimire, S. Maharjan, Adhesive small bowel obstruction: a review, JNMA J. Nepal. Med. Assoc. 61 (260) (2023) 390–396, https://doi.org/10.31729/jnma.8134.

[52] C. Li, H. Wang, H. Liu, J. Yin, L. Cui, Z. Chen, The prevention effect of poly (L-glutamic acid)/chitosan on spinal epidural fibrosis and peridural adhesion in the post-laminectomy rabbit model, Eur. Spine J. 23 (11) (2014) 2423–2431, https://doi.org/10.1007/s00586-014-3438-0.

[53] H.J. Kim, H. Kang, M.K. Kim, S.S. Han, The effects of barrier agents in postoperative pelvic adhesion formation: a comparative study of a temperature-sensitive poloxamer-based solution/gel and a hyaluronic acid-based solution in a rat uterine horn model, J. Laparoendosc. Adv. Surg. Tech. A. 28 (2) (2018) 134–139, https://doi.org/10.1089/lap.2017.0404.